Electronic Supplementary Material (ESI) for ChemComm.

Supporting Information

3D structure determination of a protein in living cells using paramagnetic NMR spectroscopy

Bin-Bin Pan[a], Feng Yang[a], Yansheng Ye[c], Qiong Wu[c], Conggang Li[c*], Thomas Huber[b*], Xun-Cheng Su[a*]

[a]State Key Laboratory of Elemento-Organic Chemistry, Collaborative Innovation Center of Chemical Science and Engineering (Tianjin), Nankai University, Tianjin 300071, China

[b]Research School of Chemistry, Australian National University, Canberra, ACT 0200, Australia

[c]Key Laboratory of Magnetic Resonance in Biological Systems, State Key Laboratory of Magnetic Resonance and Atomic and Molecular Physics, National Center for Magnetic Resonance in Wuhan, Wuhan Institute of Physics and Mathematics, Chinese Academy of Sciences, Wuhan 430071, China

S. 1 Experimental section

S. 1.1 Protein expression and purification

All oligonucleotides used for mutagenesis were purchased from Promega. $^{15}NH_4Cl$ was purchased from Aldrich-Sigma ISO-TECH. The plasmid for expression of the target protein was constructed using a PET3a vector for expression under control of the T7 promoter. *E coli* BL21 (Rosetta) strain was used for protein expression.

Recombinant GB1 and the mutants were cloned into the PET3a vector and the proteins were expressed in *E. coli* with induction by isopropyl-D-1-thiogalactopyranoside (IPTG). ^{15}N-labeled protein was prepared by growing cells in M9 medium following an established high cell-density protocol.[1] The protein was first purified through a DEAE column, and the high-salt fractions containing the target protein were collected and concentrated. Pure protein was obtained through G50 gel filtration. Approximately 28 mg of purified uniformly ^{15}N-labeled protein was obtained from 250 mL M9 medium.

S1. 2 Protein ligation: site-specifically labeling of GB1 with a paramagnetic tag (Scheme S1)

1.0 mL 2.0 mM ^{15}N-GB1 T11C (or V21C) in 20 mM tris (hydroxymethyl) aminomethane (Tris) buffer was mixed with 5 equivalents of 4PhSO_2-PyMTA tag (in 50 mM stock of aqueous solution) and 0.3 mM tris(2-carboxyethyl)phosphine (TCEP), and the pH was adjusted to 8.0. The reaction was monitored by recording ^{15}N-HSQC spectra. After overnight incubation at room temperature (about 17 h), excess of free paramagnetic tags was removed using a short PD-10 desalting column. The ligation product can also be purified by FPLC through an anion exchange column to remove the unmodified protein and excess of free tags. The PD-10 column, however, can not separate the protein-PyMTA adduct from the unmodified protein. The V21C mutant shows lower reactivity towards 4PhSO_2-PyMTA tag than

T11C and higher pH (8.5-9.0) and increase of incubation temperature (35°C) or incubation time (24 h) was necessary to get high yield of ligation product. The overall yield of ligated protein was about 80%.

S1. 3 Sample preparation for in vitro NMR

NMR samples for *in vitro* NMR measurements generally contained 0.10 mM or 0.15 mM ^{15}N-GB1 T11C (or V21C)-PyMTA in 20 mM MES buffer at pH 6.5 (the concentration of protein-PyMTA could not be correctly measured by UV absorption and the concentration was estimated by comparison of the first FIDs of ^{15}N-HSQC spectra between free GB1 and GB1-PyMTA adduct). The lanthanide complex of GB1 T11C (or V21C)-PyMTA was prepared by titration of lanthanide ion (10 mM stock in aqueous solution at pH ~5.0) into the solution of GB1-PyMTA adduct. With increasing concentration of lanthanide ion, ^{15}N-HSQC spectra were performed with each titration. Generally, the ^{15}N-HSQC spectra were recorded at molar ratio of [Ln^{3+}]/[protein] 0, 0.3, 0.6, 0.9 and 1.2, respectively. Because excess of lanthanide ion binds to the surface of GB1 non-specifically and produces solvent PREs, the NMR spectra of protein samples with [Ln^{3+}]/[protein] ratio of 0.9 were analyzed in detail.

S1.4 GB1-PyMTA samples for in *Xenopus laevis* oocytes NMR

The *in cell* NMR sample preparation was based on the previously established protocol.[3-4]

The 0.15 mM ^{15}N-labeled GB1 T11C (or V21C)-PyMTA adduct (about 550 µL) was first titrated with lanthanide ion (in 10 mM stock) with increasing the molar ratio of [Ln^{3+}]/[protein]. The ^{15}N-HSQC spectra were recorded accordingly. The solution of protein-PyMTA complexed with about 0.9 equivalent of lanthanide ion was lyophilized and then dissolved in 25 µL MilliQ water without further adjusting the pH. The protein concentration for micro-injection was typically about 3 mM. Each oocyte was injected with ~30 nL of ~3 mM ^{15}N-enriched proteins via an IM-300 microinjector

(Narishige Co. Ltd., Tokyo, Japan). Injected oocytes (about 200) were put into a 5 mm Shigemi NMR tube that contained ND96 buffer (96 mM NaCl, 2 mM KCl, 1.8 mM $CaCl_2$, 1 mM $MgCl_2$, 5 mM HEPES, pH 7.4) plus 10% D_2O. After the in-cell NMR experiments, about 200 uL of buffer above the oocytes was suctioned for a protein leakage test. No leakage was observed after NMR measurement.

S. 1.5 NMR experiments

All NMR experiments were performed on a Bruker Avance 600 NMR spectrometer equipped with a QCI-cryoprobe. All NMR spectra were collected at 298 K.

^{15}N-HSQC spectra were recorded with a spectral width of 16 and 35 ppm for proton and nitrogen dimensions, respectively. The total acquisition time applied in the ^{15}N-dimension was 46 and 29 ms, respectively, for the *in vitro* and *in-cell* ^{15}N-HSQC experiment.

For the *in vitro* experiment, a standard pulse sequence with watergate and no sensitivity-enhancement was applied and 1 s of recycle delay was used. Extract data were recorded with 16 transients and 1024 (proton) x 100 (nitrogen) complex points for ^{15}N-HSQC spectra.

For the *in-cell* experiment, water suppression was applied as trim pulse during the INEPT transfer and no sensitivity-enhancement in the pulse sequence was used and 1 s of recycle delay was applied. Extract data were recorded with 48 transients and 1024 (proton) x 64 (nitrogen) complex points for ^{15}N-HSQC spectra.

The total acquisition time for one ^{15}N-HSQC spectrum was about 1 h for *in vitro* and 2 h for *in cell* experiment, respectively. The NMR data were processed with Topspin 2.1 and analyzed with Sparky.[2] PCSs were calculated as the chemical shift differences of backbone amide protons between the paramagnetic and diamagnetic samples.

S. 1.6 GPS-Rosetta structural calculation

The GPS-Rosetta approach is based on Rosetta's *ab-initio* structure calculation. The Rosetta *ab initio* sampling algorithm used Monte-Carlo assembly of nine and three residue fragment which were generated from the primary amino acid sequence of the target protein using the Robetta server.[5] Fragment libraries that explicitly excluded the homologs of GB1 and a total of 201 PCSs measured for the backbone amide protons including 42 and 39 from GB1 T11C-PyMTA with Tm^{3+} and Yb^{3+}, 38, 40 and 42 from GB1 V21C-PyMTA with Tb^{3+}, Tm^{3+} and Yb^{3+}, respectively, were applied in the structural calculations using the previously established GPS-Rosetta protocol.[6] PCS fit quality scores for each of the metal centers were independently weighted relative to the Rosetta low-resolution scoring function and the total weight sum score S_{total} was added to the low-resolution energy function of Rosetta. The weighting factor (w) for each of the two metal centers was calculated by generating 1000 structures using Rosetta without PCS restraints using:

$$w = \left(\frac{a_{high} - a_{low}}{c_{high} - c_{low}} \right) / 2$$

where a $_{high}$ and a_{low} are the averages of the highest and lowest 10% of the values of the Rosetta *ab inito* score and c_{high} and c_{low} are the averages of the highest and lowest 10% of the PCS score value obtained by rescoring 1000 decoys with a unity PCS weighting factor.

A total of 5000 structures were calculated using GPS-Rosetta. The models were rescored with both the Rosetta all-atom energy function and weighted PCS energy, and the structures with lowest combined energy scores were selected as final structures.

Results from CS-Rosetta calculations on GB1 without PCS restraints for comparison were previously reported by us.[7]

S2. Supplementary Figures and Tables

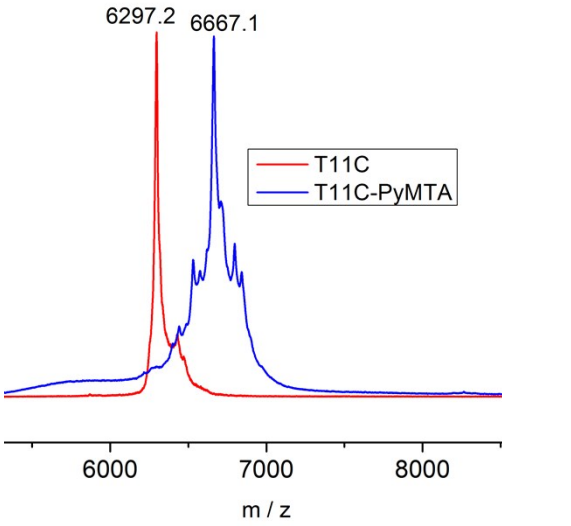

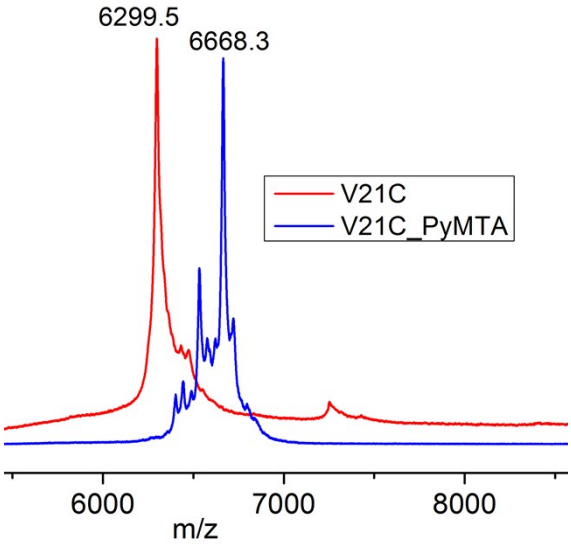

Fig. S1 MALDI-TOF mass spectra of GB1 mutant (red) and GB1-PyMTA conjugate (blue). The molecular masses of the ^{15}N-labelled protein samples are indicated. The experiment was performed for the ^{15}N-labelled GB1 mutant and its PyMTA conjugate that was purified using anion exchange chromatography. The theoretical molecular mass difference between the GB1 mutant and its PyMTA conjugate is 369 Dalton.

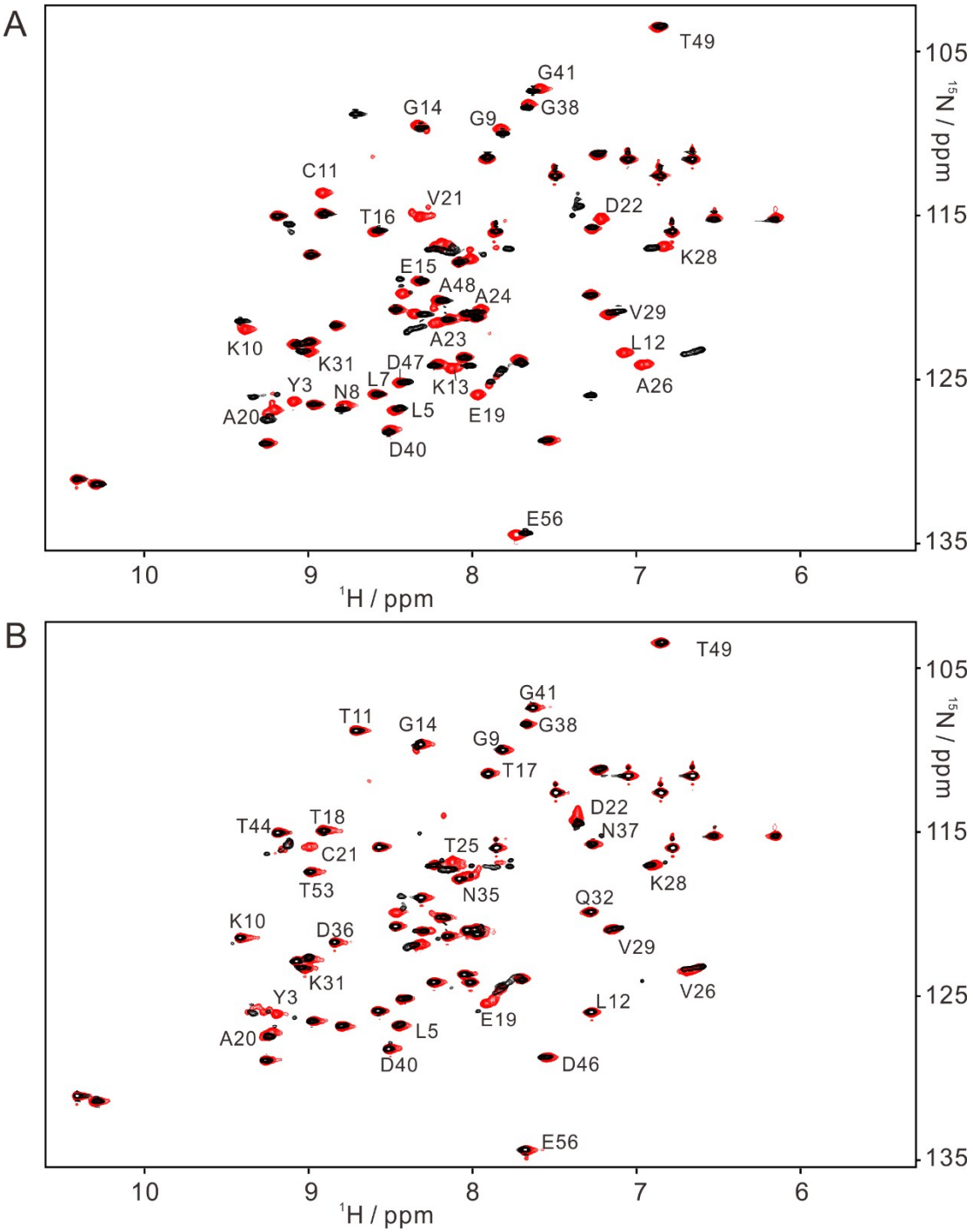

Fig. S2 Superimposition of ^{15}N-HSQC spectra of samples of 0.15 mM solutions of the ^{15}N-labeled GB1 mutants (red) and GB1-PyMTA (black). A) T11C-PyMTA. B) V21C-PyMTA. Residues are identified by labels. NMR spectra were recorded for protein samples in 20 mM MES buffer, pH 6.5, at 298 K and at a proton frequency of 600 MHz.

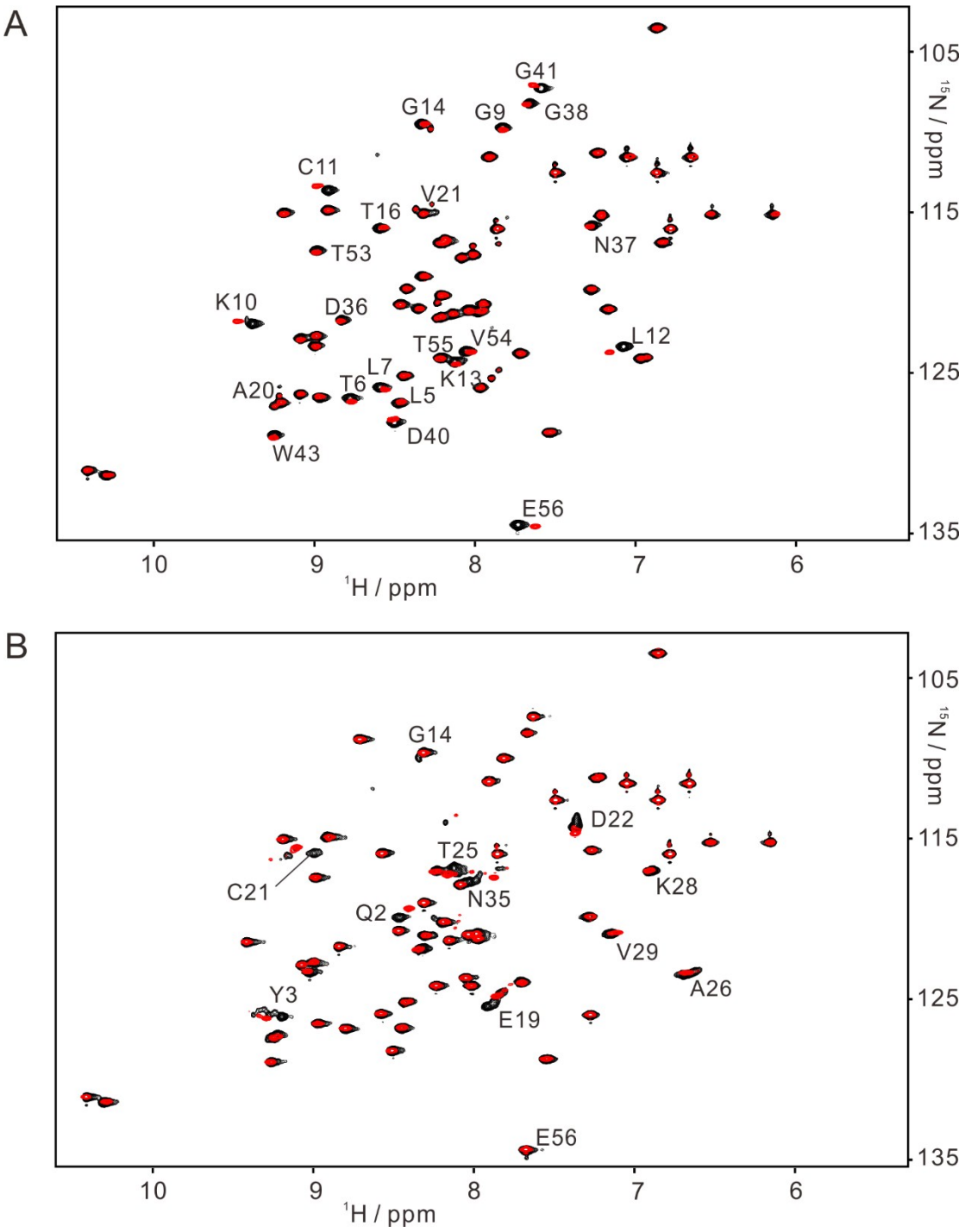

Fig. S3 Superimposition of ^{15}N-HSQC spectra of samples of 0.15 mM solutions of the ^{15}N-labeled GB1 mutant (black) and the complex of GB1-PyMTA and Y^{3+} (red). A) T11C. B) V21C. Residues showing obvious chemical shift differences are labeled. The NMR condition was the same as in Fig. S2.

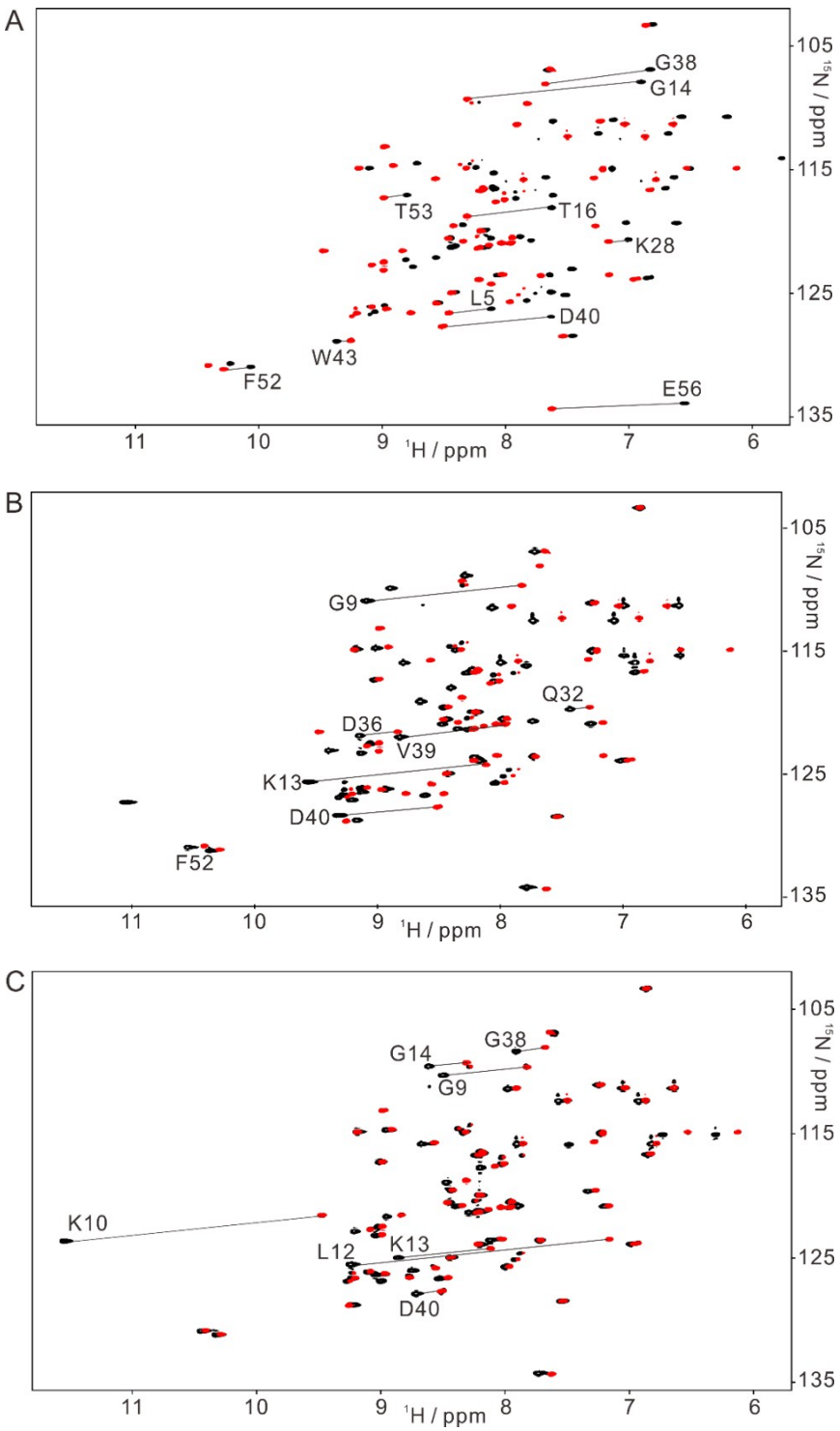

Fig. S4 Superimposition of ^{15}N-HSQC spectra of 0.10 mM solutions of the ^{15}N-labeled GB1 T11C-PyMTA complexed with about one equivalent of Y^{3+} (red) and paramagnetic lanthanide (black), respectively. A) Tb^{3+}. B) Tm^{3+}. C) Yb^{3+}. The cross-peaks corresponding to the paramagnetic and diamagnetic species was connected with solid lines. The NMR condition was the same as in Fig. S2.

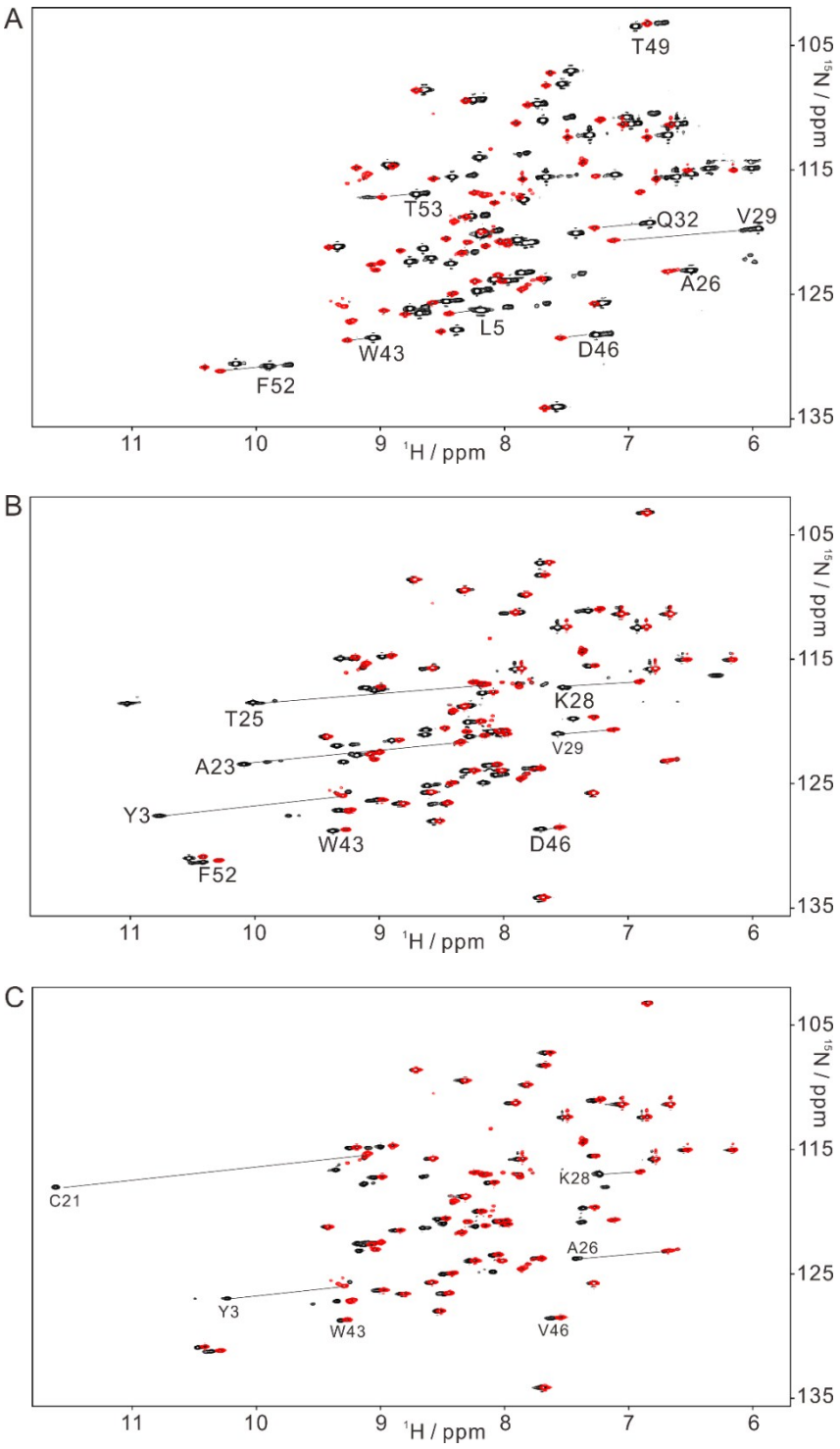

Fig. S5 Superimposition of ^{15}N-HSQC spectra of samples of 0.15 mM solutions of the ^{15}N-labeled GB1 V21C-PyMTA complexed with one equivalent of Y^{3+} (red) and paramagnetic lanthanide (black), respectively. A) Tb^{3+}. B) Tm^{3+}. C) Yb^{3+}. The cross-peaks corresponding to the paramagnetic and diamagnetic species was connected with solid lines. The additional diamagnetic peaks in the paramagnetic samples of Tb^{3+}, Tm^{3+} and Yb^{3+} complexes are due to the insufficient addition of paramagnetic ions. The NMR condition was the same as in Fig. S2.

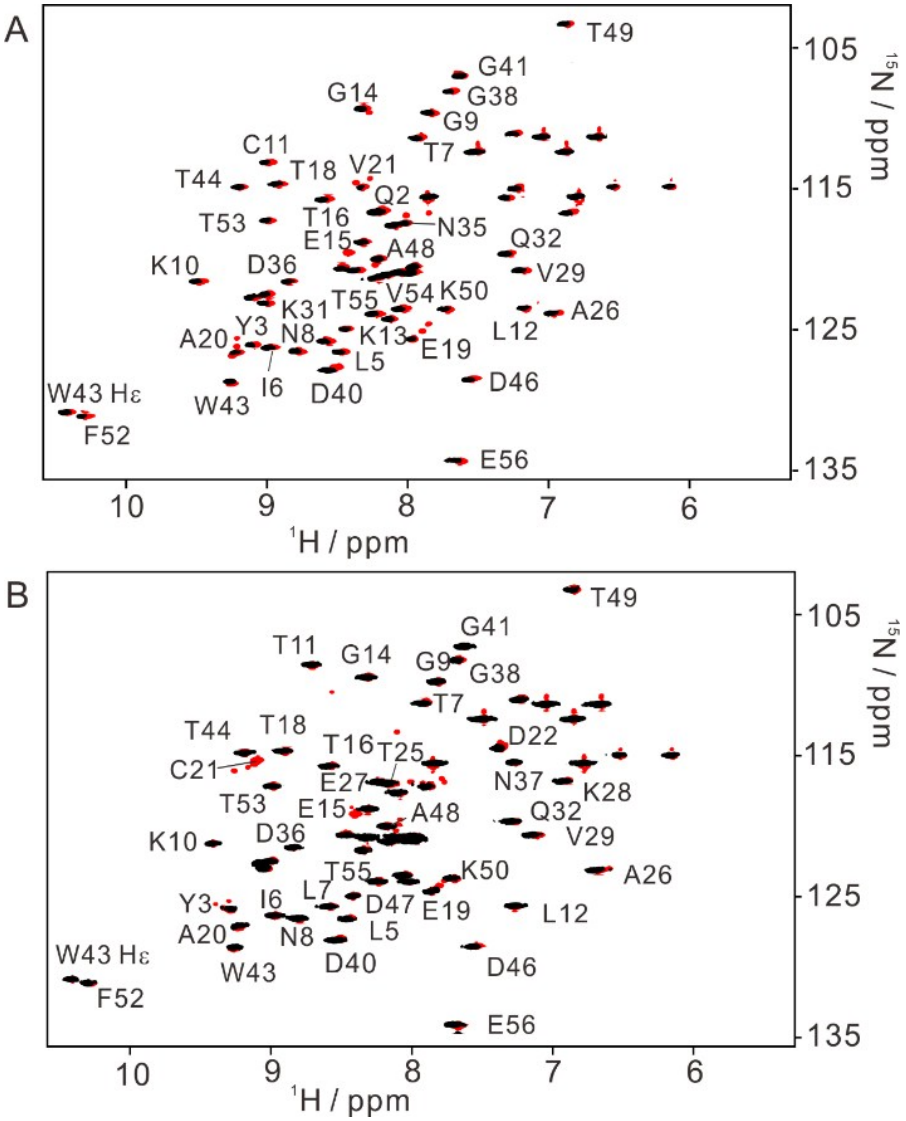

FigS. 6 Superimposition of ^{15}N-HSQC spectra of 0.10 mM GB1-PyMTA complexed with about 1.0 equivalent of Y^{3+} recorded in 20 mM MES buffer at pH 6.5 (red) and in living *Xenopus laevis* oocytes (black) at 298 K. A) T11C-PyMTA. B) V21C-PyMTA. The cross-peaks are identified with residue labels.

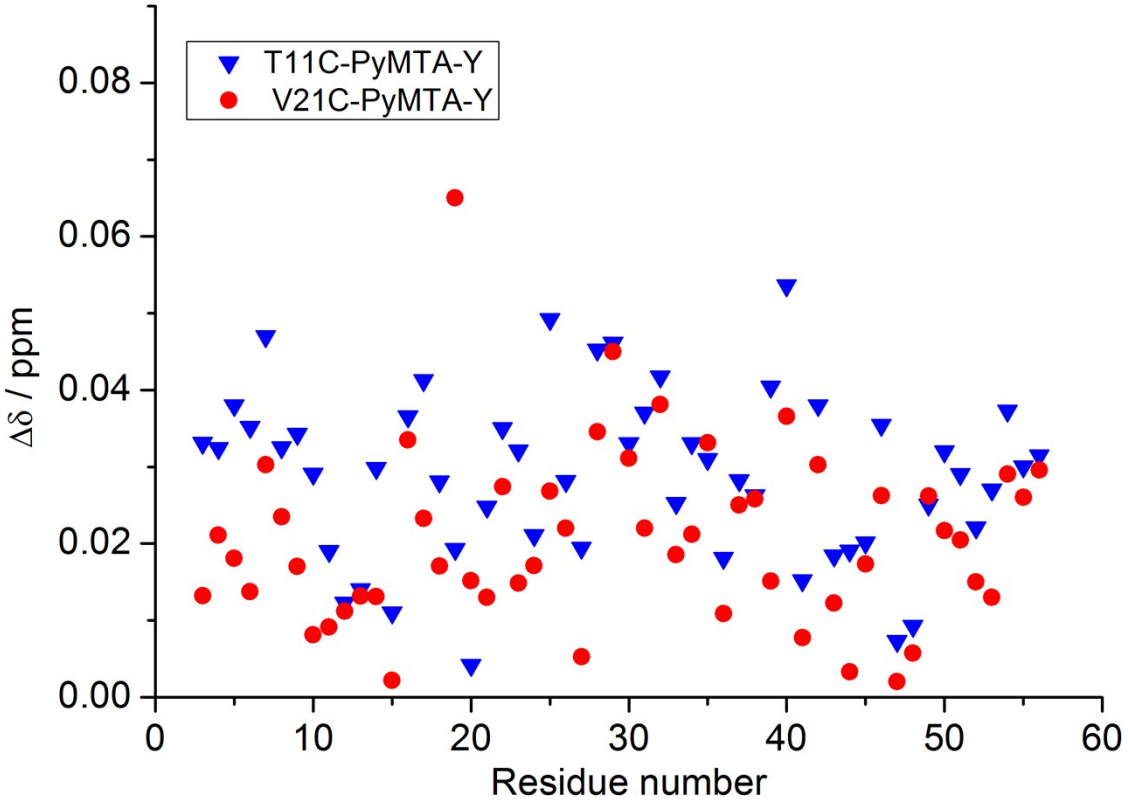

Fig. S7 Plot of chemical shift differences as a function of amino acid sequence for protein samples measured in vitro and in cell. Protein samples GB1 T11C-PyMTA (triangle) and GB1 V21C-PyMTA (circle) complexed with diamagnetic Y^{3+} were measured in 20 mM MES buffer at pH 6.5 and in *Xenopus laevis* oocytes at 298 K, respectively. Chemical shift differences were calculated as $\Delta\delta = \mathrm{Sqrt}[(\Delta\delta_H)^2 + (\Delta\delta_N/10)^2]$, where $\Delta\delta_H$ and $\Delta\delta_N$ are the backbone amide chemical shift differences in the hydrogen and nitrogen dimension, respectively.

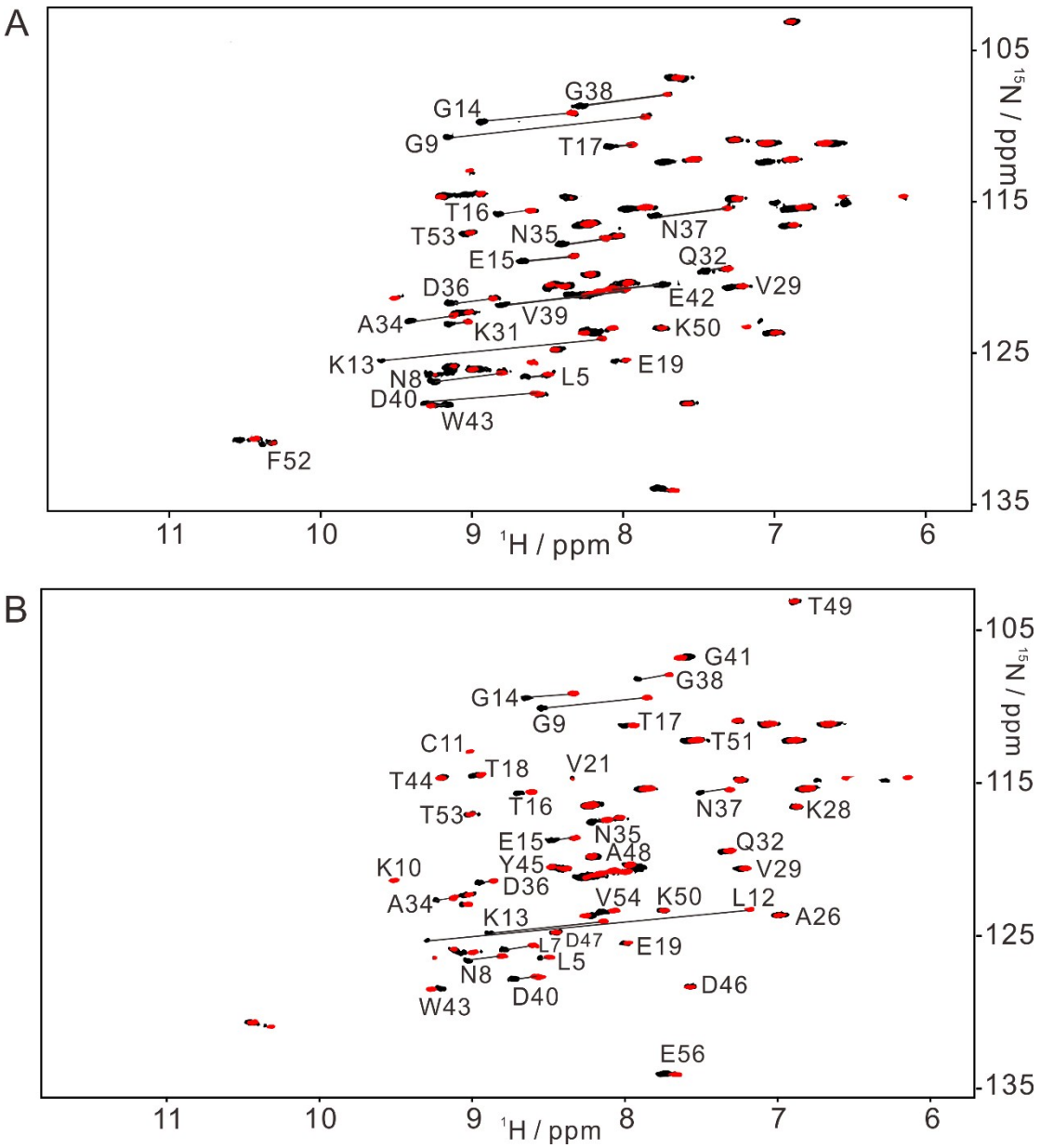

Fig. S8 Superimposition of ^{15}N-HSQC spectra of ^{15}N-labeled GB1 T11C-PyMTA complexed with Y^{3+} (red) and paramagnetic lanthanide (black), respectively, measured in *Xenopus laevis* oocytes at 298K with a proton frequency of 600 MHz. A) Tm^{3+}. B) Yb^{3+}. The cross-peaks corresponding to the paramagnetic and diamagnetic species were connected with solid lines. In the sample of T11C-PyMTA complexed with Tm^{3+}, the protein was not fully saturated with paramagnetic ion due to insufficient addition of Tm^{3+} during the sample preparation.

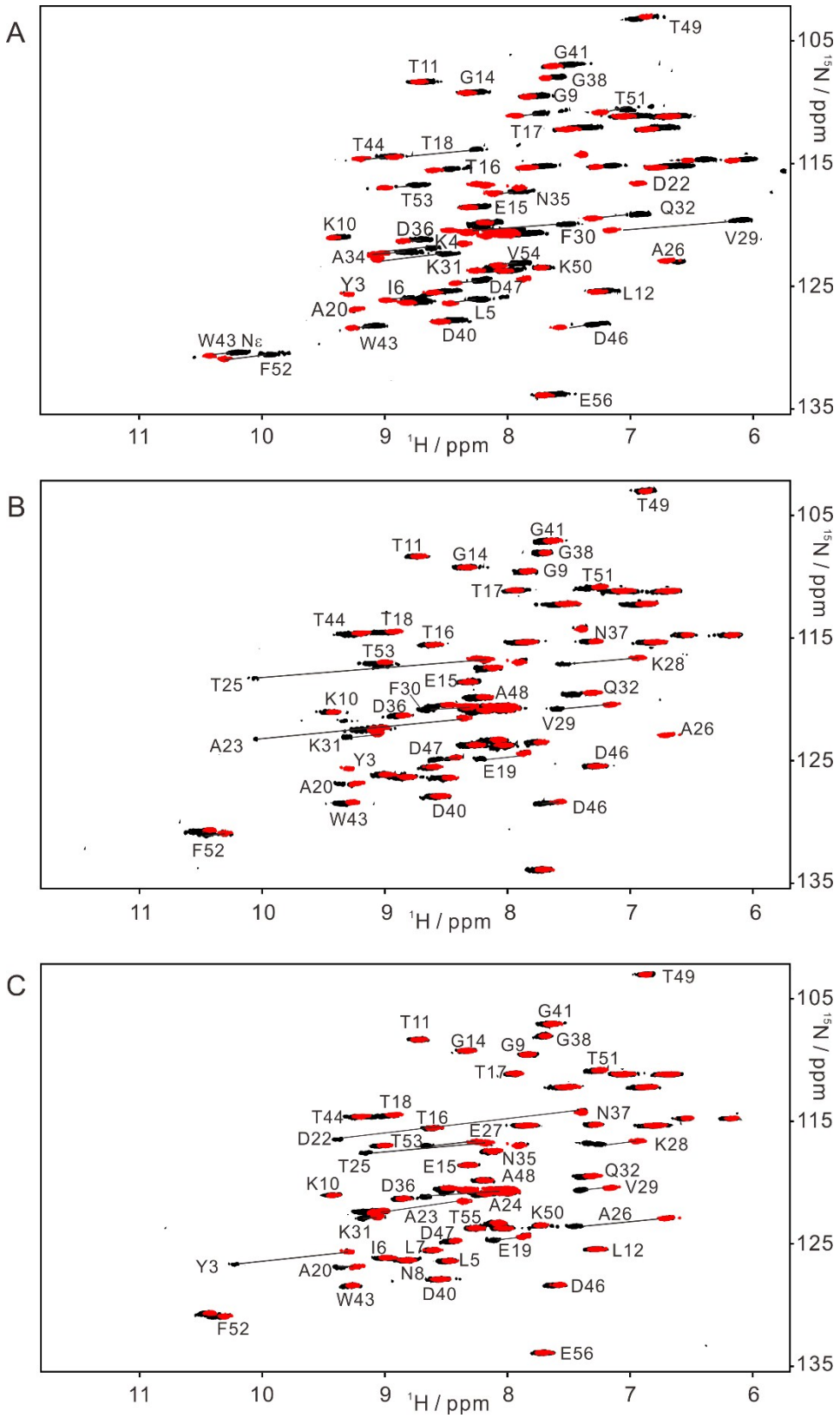

Fig. S9 Superimposition of ^{15}N-HSQC spectra of ^{15}N-labeled GB1 V21C-PyMTA complexed with Y^{3+} (red) and paramagnetic lanthanide ion (black), respectively, measured in *Xenopus laevis* oocytes at 298K with a proton frequency of 600 MHz. The cross-peaks corresponding to the paramagnetic and diamagnetic species were connected with solid lines. A) Tb^{3+}. B) Tm^{3+}. C) Yb^{3+}.

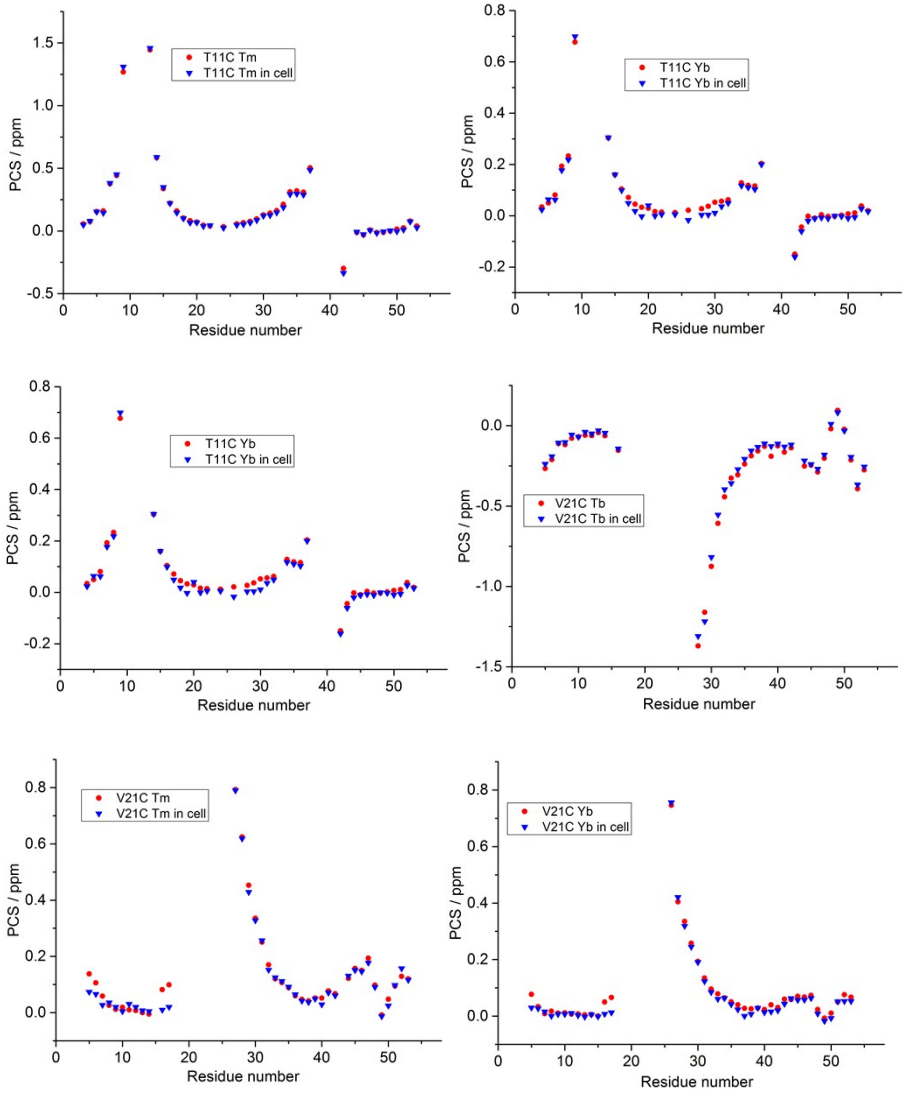

Fig. S10 The plot of PCS as a function of amino acid sequence. PCSs of backbone amide protons were measured for the complexes of GB1-PyMTA and paramagnetic lanthanide ions in 20 mM MES buffer at pH 6.5 and in *Xenopus laevis* oocytes, respectively, at 298 K.

Table S1. $\Delta\chi$-tensor parameters of GB1-PyMTA adducts in complex with paramagnetic lanthanide ions determined in 20 mM MES at pH 6.5 and in *Xenopus laevis* oocytes, respectively.[a]

GB1	Ln^{3+}	$\Delta\chi_{ax}$[b]	$\Delta\chi_{rh}$[b]	Q-factor(%)	α[c]	β[c]	γ[c]
T11C	Tb^{3+}	6.1	3.6	4.0	21.0	94.8	35.9
	Tm^{3+}	3.4 (-2.8)	1.9 (-1.8)	5.0 (7.0)	120.7 (28.8)	45.8 (96.9)	8.8 (42.4)
	Yb^{3+}	-2.9(-1.7)	-0.8 (-0.2)	11.4 (11.7)	17.9 (15.9)	101.8 (96.5)	136.7 (172.3)
V21C	Tb^{3+}	12.0 (-7.8)	7.9 (-3.5)	5.0 (5.0)	51.8 (128.5)	128.8 (77.8)	11.7 (32.9)
	Tm^{3+}	-6.5 (5.1)	-4.4 (3.2)	13.0 (8.0)	64.9 (147.9)	136.5 (80.4)	13.1 (51.2)
	Yb^{3+}	3.0 (1.9)	1.9 (0.4)	11.0 (13.0)	135.7 (132.7)	84.4 (80.7)	24.8 (42.9)

[a]The tensor parameters (in UTR convention) were obtained by fitting the PCS data of backbone amide protons to the crystal structure of GB1 (PDB code:2QMT). The tensor parameters obtained in *Xenopus laevis* oocytes are shown in brackets. PCSs of residues 38-41 and 54-56 that are close to T11C were excluded in the fitting of T11C-PyMTA adduct and those of residues 3-4, 17-27 and 54-56 were excluded in the fitting of V21C-PyMTA adduct. [b] In units of 10^{-32} m^3. [c] In degrees relative to the crystal structure of GB1 (PDB code: 2QMT).

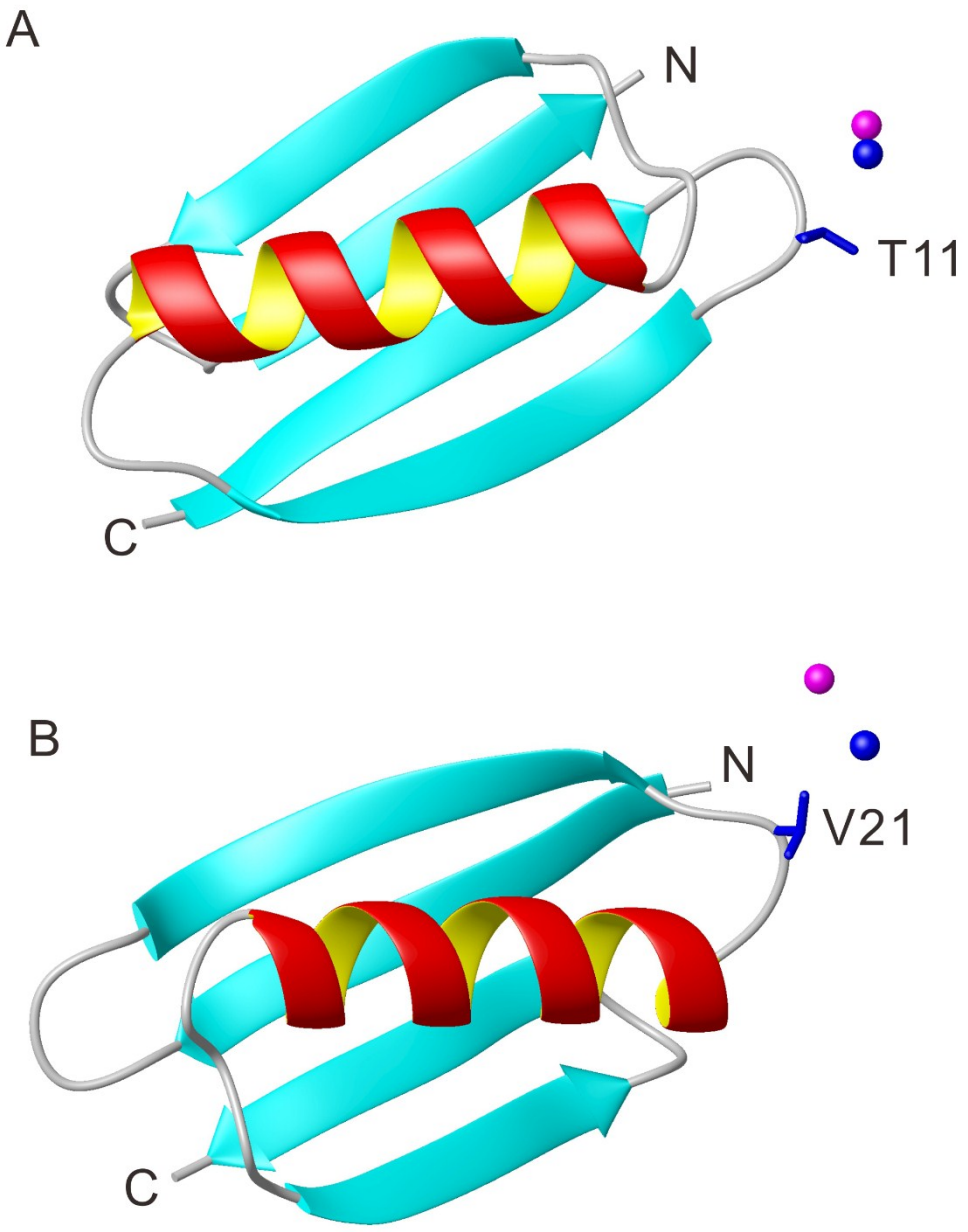

Fig. S11 Ribbon structural representation of GB1 with respect to the paramagnetic center calculated using the experimental PCSs from in vitro (blue sphere) and in *Xenopus laevis* oocytes (magenta sphere), respectively. A) T11C-PyMTA. B) V21C-PyMTA.

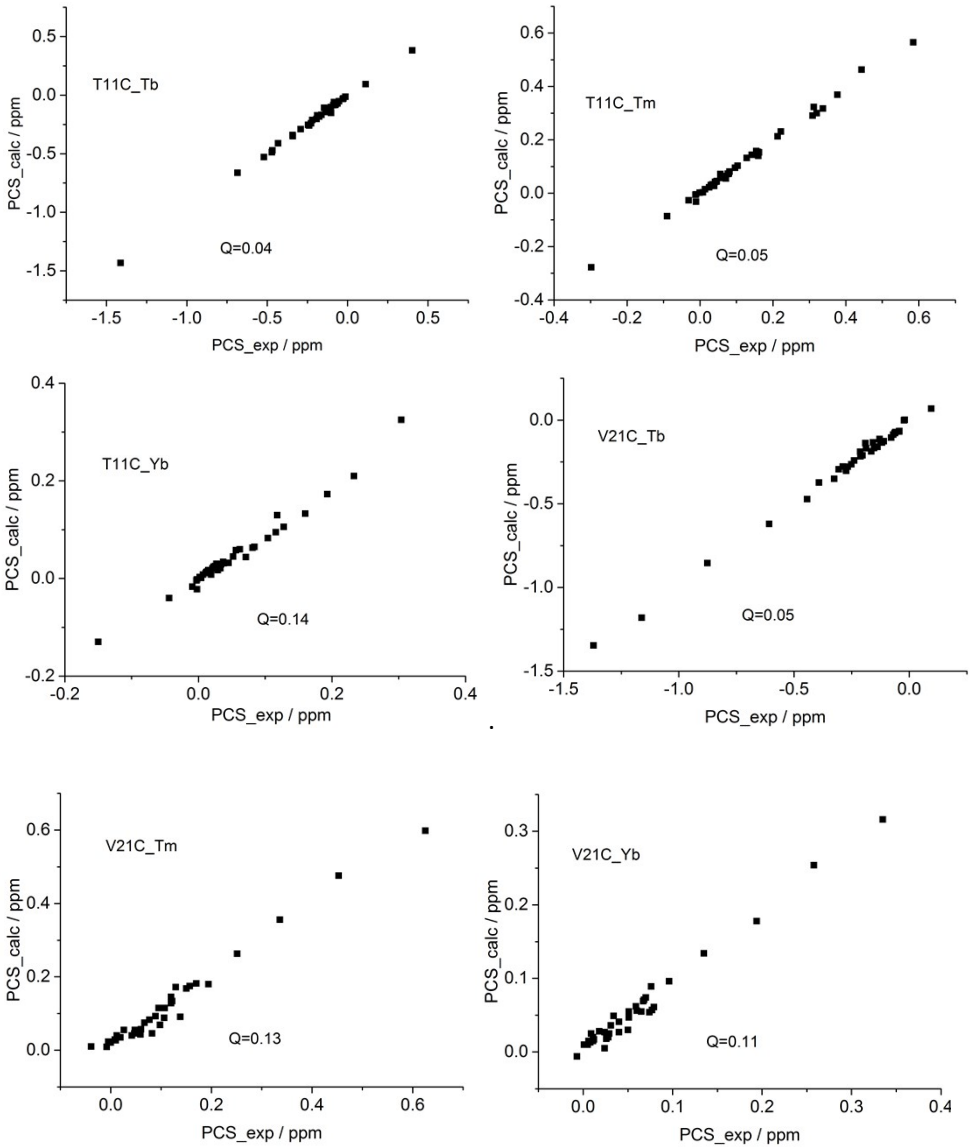

Fig. S12 Correlations of the experimental PCSs (PCS_exp) and back-calculated PCSs (PCS_calc) using Numbat program. Quality factors ($Q=\mathrm{sqrt}\{\Sigma(PCS_i^{calc}-PCS_i^{exp})^2\}/\mathrm{sqrt}\{\Sigma(PCS_i^{exp})^2\}$)are shown as insert in figure. PCSs were measured for the protein samples of GB1-PyMTA complexed with paramagnetic lanthanide in 20 mM MES buffer at pH 6.5 and 298 K.

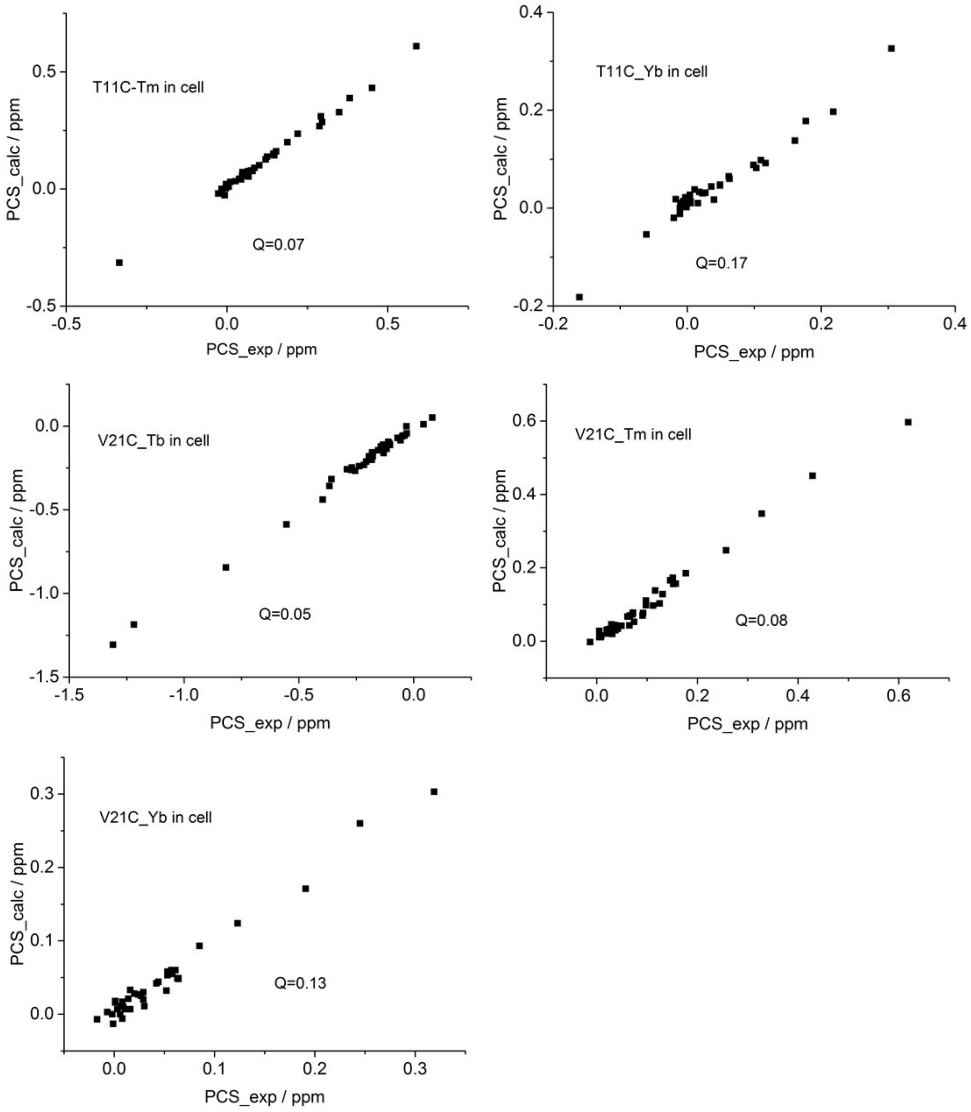

Fig. S13 Correlations of the experimental PCSs (PCS_exp) and back-calculated PCSs (PCS_calc) using Numbat program. Quality factors ($Q=\mathrm{sqrt}\{\Sigma(PCS_i^{calc}-PCS_i^{exp})^2\}/\mathrm{sqrt}\{\Sigma(PCS_i^{exp})^2\}$) are shown as insert in figure. PCSs were measured for the protein samples of GB1-PyMTA complexed with paramagnetic lanthanide in *Xenopus laevis* oocytes and at 298 K.

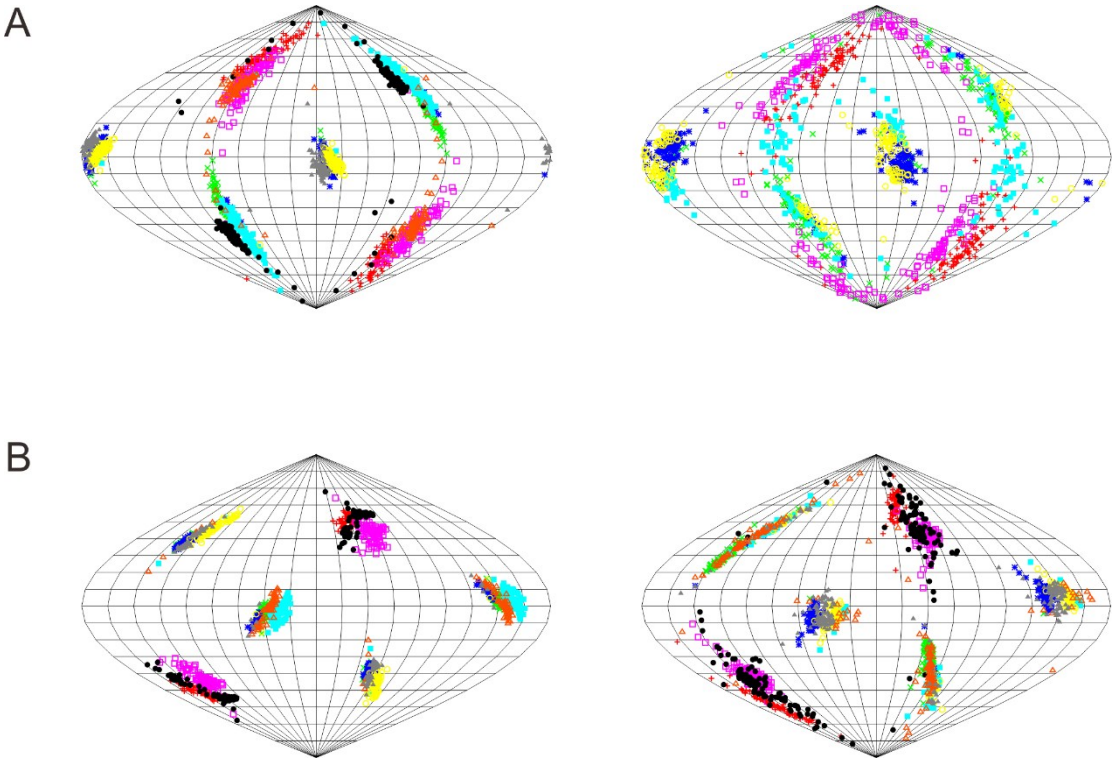

Fig. S14 Sanson-Flamsteed projection plots comparing the orientations of the principal axes, z, x and y, of the $\Delta\chi$-tensors determined for GB1-PyMTA conjugates in complex with paramagnetic lanthanide ions by randomly selecting and simultaneous fitting 80% of the PCS data (used for tensor determination in Table 1) measured in vitro (left panel) and in cell (right panel) to the crystal structure of GB1 (PDB code: 2QMT), respectively. A) T11C-PyMTA. B) V21C-PyMTA.

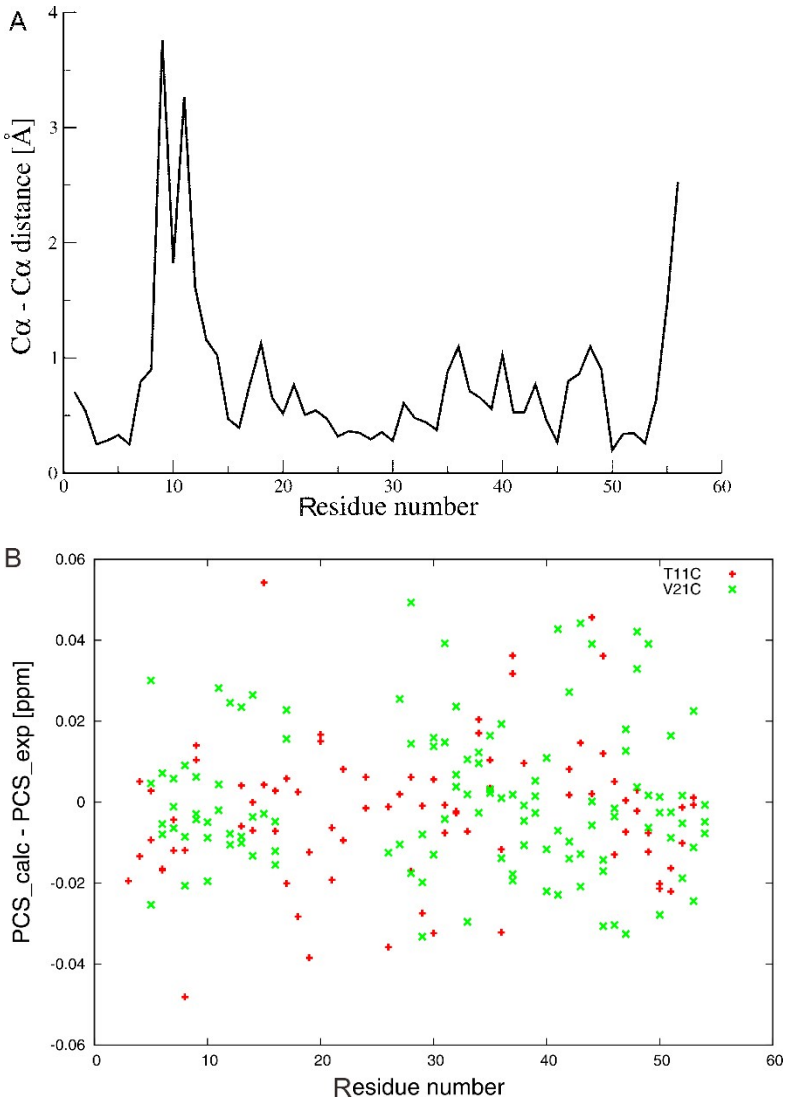

Fig. S15 Structural comparison between the GPS-Rosetta calculated structure of GB1 using PCS measured in living cells and the crystal structure. A) The Cα displacement between the lowest energy structure calculated from GPS-Rosetta using in-cell PCS and the crystal structure (Pdb code:2QMT). B) PCS deviations between the experimental and back-calculated data from the lowest energy structure of GB1 that was calculated from GPS-Rosetta.

Table S2. PCSs of backbone amide protons measured for GB1 T11C-PyMTA adduct complexed with Tb^{3+}, Tm^{3+}, and Yb^{3+} in 20 mM MES (pH 6.5) and in *Xenopus laevis* oocytes at 298 K, respectively.

	Tb^{3+}		Tm^{3+}		Yb^{3+}	
Residue	in vitro (ppm)	in cell (ppm)	in vitro (ppm)	in cell (ppm)	in vitro (ppm)	in cell (ppm)
Y3	-0.102		0.056	0.048		
K4	-0.177		0.076	0.079	0.034	0.023
L5	-0.341		0.154	0.153	0.05	0.063
I6			0.16	0.144	0.081	0.062
L7			0.377	0.382	0.193	0.177
N8			0.443	0.451	0.233	0.218
G9			1.268	1.31	0.677	0.699
K13			1.445	1.459		0.745
G14	-1.412		0.585	0.589	0.304	0.305
E15	-0.685		0.337	0.349	0.16	0.161
T16	-0.471		0.222	0.22	0.104	0.099
T17	-0.291		0.159	0.145	0.071	0.049
T18	-0.193		0.103	0.1	0.045	0.018
E19	-0.137		0.081	0.066	0.033	-0.003
A20	-0.145		0.071	0.067	0.029	0.04
V21	-0.079		0.046	0.038	0.016	0.01
D22	-0.076		0.041	0.044	0.014	0.005
A23						
A24	-0.063		0.034	0.025	0.012	0.005
T25	-0.088					
A26	-0.108		0.056	0.047	0.021	-0.017
E27	-0.115		0.065	0.052	0.027	0.003
K28	-0.125		0.076	0.066	0.025	0.003
V29	-0.162		0.096	0.085	0.037	0.004
F30	-0.227		0.128	0.12	0.052	0.011
K31	-0.239		0.142	0.125	0.056	0.036
Q32	-0.245		0.162	0.147	0.062	0.049
Y33	-0.342		0.213	0.188	0.084	
A34	-0.521		0.312	0.292	0.128	0.117
N35	-0.468		0.32	0.296	0.118	0.11
D36	-0.432		0.309	0.288	0.116	0.103
N37	-0.775		0.504	0.486	0.204	0.2
E42	0.402		-0.298	-0.335	-0.15	-0.161
W43	0.112				-0.044	-0.061
T44	-0.084		-0.011	-0.007	-0.002	-0.02
Y45	-0.013		-0.031	-0.027	-0.009	-0.011

D46	-0.079	0.008	0.005	0.004	-0.008
D47	-0.026	-0.012	-0.017	-0.003	-0.011
A48	-0.029	-0.011	-0.004	-0.002	-0.002
T49	-0.053	-0.006	0.003	0.002	-0.003
K50	-0.072	0.014	-0.003	0.007	-0.01
T51	-0.103	0.025	0.01	0.011	-0.006
F52	-0.219	0.079	0.075	0.038	0.027
T53	-0.188	0.039	0.026	0.019	0.016

Table S3. PCSs of backbone amide protons measured for GB1 V21C-PyMTA adduct complexed with Tb^{3+}, Tm^{3+}, and Yb^{3+} in 20 mM MES (pH 6.5) and in *Xenopus laevis* oocytes at 298 K, respectively.

	Tb^{3+}		Tm^{3+}		Yb^{3+}	
Residue	in vitro (ppm)	In cell (ppm)	in vitro (ppm)	in cell (ppm)	in vitro (ppm)	in cell (ppm)
K4						
L5	-0.267	-0.238	0.138	0.074	0.077	0.03
I6	-0.211	-0.191	0.106	0.066	0.034	0.027
L7	-0.111	-0.106	0.059	0.027	0.009	0.016
N8	-0.118	-0.103	0.026	0.036	0.018	0.005
G9	-0.078	-0.057	0.012	0.02	0.011	0.007
K10	-0.069	-0.07	0.019	0.005	0.012	0.007
T11	-0.06	-0.039	0.01	0.031	0.008	0.011
L12	-0.062	-0.049	0.008	0.02	0.008	0.003
K13	-0.043	-0.03	0	0.008	0.005	-0.002
G14	-0.063	-0.045	-0.005	0.005	0.006	0.006
E15					0.01	0.01
T16	-0.153	-0.143	0.082	0.01	0.05	0.008
T17			0.099	0.02	0.066	0.013
A26					0.746	0.756
E27			0.793	0.79	0.405	0.421
K28	-1.37	-1.309	0.625	0.619	0.335	0.319
V29	-1.161	-1.218	0.453	0.429	0.258	0.245
F30	-0.876	-0.818	0.336	0.328	0.194	0.191
K31	-0.608	-0.554	0.251	0.257	0.135	0.123
Q32	-0.443	-0.396	0.17	0.152	0.096	0.085
Y33	-0.326	-0.358	0.12	0.125	0.079	0.061
A34	-0.306	-0.272	0.107	0.112	0.065	0.064
N35	-0.239	-0.207	0.089	0.092	0.051	0.042
D36	-0.187	-0.155	0.06	0.065	0.04	0.024
N37	-0.157	-0.133	0.047	0.042	0.028	0.01
G38	-0.129	-0.111	0.042	0.037	0.026	0.008
V39	-0.19	-0.128	0.052	0.049	0.029	0.029
D40	-0.126	-0.112	0.052	0.029	0.024	0.014
G41	-0.165	-0.131	0.077	0.071	0.04	0.016
E42	-0.138	-0.118	0.067	0.061	0.031	0.02
W43	-0.221	-0.183			0.06	0.044
T44	-0.251	-0.217	0.122	0.131	0.059	0.063
Y45	-0.245	-0.24	0.157	0.151	0.07	0.057
D46	-0.288	-0.269	0.15	0.146	0.068	0.058
D47	-0.203	-0.181	0.194	0.177	0.074	0.064

A48	-0.02	0.01	0.098	0.091	0.024	0.009
T49	0.095	0.081	-0.008	-0.013	-0.007	-0.017
K50	-0.023	-0.032	0.048	0.025	0.011	-0.007
T51	-0.213	-0.195	0.095	0.098	0.051	0.052
F52	-0.392	-0.367	0.129	0.157	0.076	0.053
T53	-0.275	-0.255	0.12	0.116	0.067	0.053
V54	-0.190	-0.178	0.068	0.719	0.027	0.029

S. 3. Supplementary Reference

1. Cao C., Chen J. L., Yang Y., Huang F., Otting G., Su X. C. *J. Biomol. NMR* **2014**, *59*, 251-261.
2. Goddard T. D., Kneller D. G. Sparky 3, University of California, San Francisco
3. Selenko C, Serber Z, Gadea B, Ruderman J, Wagner G. *Proc. Natl. Acad. Sci. USA* **2006**, *103*, 11904-11905.
4. a) Ye Y., Liu X., Xu G., Liu M., Li C. *Angew. Chem. Int. Ed. Engl.* **2015**, *54*, 5328-5330. b) Ye Y., Liu X., Chen Y., Xu G., Wu Q., Zhang Z., Yao C., Liu M., Li C. *Chem. Eur. J.* **2015**, *21*, 8686-8690
5. Kim D. E, Chivian D., Baker D. *Nucleic Acids Res.* **2004**; *32*, W526–531.
6. Pilla K. B., Leman J. K., Otting G., Huber T. *PLoS One* **2015**, *10*, e0127053.
7. Schmitz C., Vernon R., Otting G., Baker D., Huber T. *J. Mol. Biol.* **2012**, *416*, 668-677.